Preparation, Characterization, Redox Properties, and UV−Vis−NIR Spectra of Binuclear Ruthenium Complexes $[\{(Phtpy)(PPh_3)_2Ru\}_2\{C{\equiv}C-(CH{=}CH)_m-C{\equiv}C\}]^{n+}$ (Phtpy = 4′-phenyl-2,2′:6′,2″-terpyridine)

Li-Bin Gao,[†] Sheng-Hua Liu,*[,‡] Li-Yi Zhang,[†] Lin-Xi Shi,[†] and Zhong-Ning Chen*[,†]

State Key Laboratory of Structural Chemistry, Fujian Institute of Research on the Structure of Matter, The Chinese Academy of Sciences, Fuzhou, Fujian 350002, China, and Key Laboratory of Pesticide & Chemical Biology, College of Chemistry, Central China Normal University, Wuhan 430079, China

Received September 4, 2005

A series of C_4-C_{10} bridged $Ru_2^{II,II}$ complexes $[\{(Phtpy)(PPh_3)_2Ru\}_2(C{\equiv}C-(CH{=}CH)_m-C{\equiv}C)]^{2+}$ (m = 0, 1, 2, 3) were prepared by reaction of $[(Phtpy)(PPh_3)_2Ru(acetone)]^{2+}$ with $Me_3Si-C{\equiv}C-(CH{=}CH)_m-C{\equiv}C-SiMe_3$ in the presence of potassium fluoride. Oxidation of the $Ru_2^{II,II}$ complexes by 1 equiv of ferrocenium hexafluorophosphate gave the stable $Ru_2^{II,III}$ mixed-valence complexes $[\{(Phtpy)(PPh_3)_2Ru\}_2(C{\equiv}C-(CH{=}CH)_m-C{\equiv}C)]^{3+}$ when m = 0, 1, or 2. These complexes were all characterized by microanalyses, ESI-MS, ^1H and ^{31}P NMR, IR, and UV−vis−NIR spectroscopy, cyclic and differential pulse voltammetry, and X-ray crystallography for compound $[\mathbf{1}](PF_6)_2$. The wave separations $\Delta E_{1/2}$ ($E_{1/2}^A - E_{1/2}^B$) due to stepwise oxidation of two Ru^{II} into Ru^{III} are 0.610, 0.260, 0.165, and <0.070 V for m = 0−3, respectively, in dichloromethane solutions, revealing a significant dependence of the electronic communication on metal−metal distances. The visible−NIR spectral studies on the $Ru_2^{II,III}$ mixed-valence complexes $[\{(Phtpy)(PPh_3)_2Ru\}_2(C{\equiv}C-(CH{=}CH)_m-C{\equiv}C)]^{3+}$ (m = 0, 1, 2) demonstrated that electronic delocalization along the molecular rods attenuates dramatically with the increase of the ethenyl number.

Introduction

Linear compounds with redox-active organometallic termini linked by π-conjugated organic ligands are of current interest as candidates for "molecular wires" that allow electron transfer to occur along the molecular backbones.[1,2] Among different approaches to construct such linear donor−spacer−acceptor assembly, the compounds with an unsaturated carbon chain spanning two organometallic components have actively been investigated.[2−6] Particular attention has been focused on investigation of bimetallic polyynediyl complexes {M}−$(C{\equiv}C)_m$−{M} (m = 1, 2, 3, etc.)[6−17] and polyylenediyl complexes {M}−

* To whom correspondence should be addressed. E-mail: czn@ms.fjirsm.ac.cn; chshliu@mail.ccnu.edu.cn.

[†] Fujian Institute of Research on the Structure of Matter.

[‡] Central China Normal University.

(1) (a) Robertson, N.; McGowan, C. A. *Chem. Soc. Rev.* **2003**, *32*, 96. (b) Launay, J.-P. *Chem. Soc. Rev.* **2001**, *30*, 386. (c) Ward, M. D. *Chem. Soc. Rev.* **1995**, *24*, 121.

(2) (a) Ren, T. *Organometallics* **2005**, *24*, 4854−4870. (b) Martin, R. E.; Diederich, F. *Angew. Chem., Int. Ed.* **1999**, *38*, 1350. (c) Paul, F.; Lapinte, C. *Coord. Chem. Rev.* **1998**, *178−180*, 431. (d) Szafert, S.; Gladysz, J. A. *Chem. Rev.* **2003**, *103*, 4175. (e) Long, N. J.; Williams, C. K. *Angew. Chem., Int. Ed.* **2003**, *42*, 2586. (f) Ziessel, R.; Hissler, M.; El-ghayoury, A.; Harriman, A. *Coord. Chem. Rev.* **1998**, *178−180*, 1251. (g) Bruce, M. I.; Low, P. J. *Adv. Organomet. Chem.* **2004**, *50*, 179. (h) Touchard, D.; Dixneuf, P. H. *Coord. Chem. Rev.* **1998**, *178−180*, 409. (i) Akita, M.; Sakurai, A.; Chung, M.-C.; Moro-oka, Y. *J. Organomet. Chem.* **2003**, *670*, 2.

(3) Field, L. D.; Turnbull, A. J.; Turner, P. *J. Am. Chem. Soc.* **2002**, *124*, 3692.

(4) Adams, R. D.; Qu, B.; Smith, M. D. *Inorg. Chem.* **2001**, *40*, 2932.

(5) (a) Zhu, Y.; Clot, O.; Wolf, M. O.; Yap, G. P. A. *J. Am. Chem. Soc.* **1998**, *120*, 1812. (b) Iyer, R. S.; Selegue, J. P. *J. Am. Chem. Soc.* **1987**, *109*, 910.

(6) (a) Hu, Q. Y.; Lu, W. X.; Tang, H. D.; Sung, H. H. Y.; Wen, T. B.; Williams, I. D.; Wong, G. K. L.; Lin, Z.; Jia, G. *Organometallics* **2005**, *24*, 3966. (b) Xia, H.; Wen, T. B.; Hu, Q. Y.; Wang, X.; Chen, X.; Shek, L. Y.; William, I. D.; Wong, K. S.; Wong, G. K. L.; Jia, G. *Organometallics* **2005**, *24*, 562

(7) (a) Rigaut, S.; Massue, J.; Touchard, D.; Fillaut, J.-L.; Golhen, S.; Dixneuf, P. H. *Angew. Chem., Int. Ed.* **2002**, *41*, 4513. (b) Uno, M.; Dixneuf, P. H. *Angew. Chem., Int. Ed.* **1998**, *37*, 1714. (c) Rigaut, S.; Perruchon, J.; Pichon, L. L.; Touchard, D.; Dixneuf, P. H. *J. Organomet. Chem.* **2003**, *670*, 37. (d) Rigaut, S.; Pichon, L. L.; Daran, J.-C.; Touchard, D.; Dixneuf, P. H. *Chem. Commun.* **2001**, 1206. (e) Rigaut, S.; Touchard, D.; Dixneuf, P. H. *J. Organomet. Chem.* **2003**, *684*, 68.

(8) (a) Bruce, M. I.; Low, P. J.; Costuas, K.; Halet, J.-F.; Best, S. P.; Heath, G. A. *J. Am. Chem. Soc.* **2000**, *122*, 1949. (b) Bruce, M. I.; Hall, B. C.; Kelly, B. D.; Low, P. J.; Skelton, B. W.; White, A. H. *J. Chem. Soc., Dalton Trans.* **1999**, 3719. (c) Bruce, M. I.; Hinterding, P.; Tiekink, E. R. T.; Skelton, B. W.; White, A. H. *J. Organomet. Chem.* **1993**, *450*, 209. (d) Bruce, M. I.; Ellis, B. G.; Low, P. J.; Skelton, B. W.; White, A. H. *Organometallics* **2003**, *22*, 3184. (e) Bruce, M. I.; Costuas, K.; Davin, T.; Ellis, B. G.; Halet, J.-F.; Lapinte, C.; Low, P. J.; Smith, M. E.; Skelton, B. W.; Toupet, L.; White, A. H. *Organometallics* **2005**, *24*, 3864.

(9) (a) Antonova, A. B.; Bruce, M. I.; Ellis, B. G.; Gaudio, M.; Humphrey, P. A.; Jevric, M.; Melino, G.; Nicholson, B. K.; Perkins, G. J.; Skelton, B. W.; Stapleton, B.; White, A. H.; Zaitseva, N. N. *Chem. Commun.* **2004**, 960. (b) Bruce, M. I.; Ellis, B. G.; Gaudio, M.; Lapinte, C.; Melino, G.; Paul, F.; Skelton, B. W.; Smith, M. E.; Toupet, L.; White, A. H. *J. Chem. Soc., Dalton Trans.* **2004**, 1601.

(10) (a) Paul, F.; Meyer, W. E.; Toupet, L.; Jiao, H.; Gladysz, J. A.; Lapinte, C. *J. Am. Chem. Soc.* **2000**, *122*, 9405. (b) Narvor, N. L.; Toupet, L.; Lapinte, C. *J. Am. Chem. Soc.* **1995**, *117*, 7129. (c) Courmarcel, J.; Gland, G. L.; Toupet, L.; Paul, F.; Lapinte, C. *J. Organomet. Chem.* **2003**, *670*, 108. (d) Guillaume, V.; Mahias, V.; Mari, A.; Lapinte, C. *Organometallics* **2000**, *19*, 1422. (e) Coat, F.; Guillevic, M.-A.; Toupet, L.; Paul, F.; Lapinte, C. *Organometallics* **1997**, *16*, 5988.

(11) (a) Dembinski, R.; Bartik, T.; Bartik, B.; Jaeger, M.; Gladysz, J. A. *J. Am. Chem. Soc.* **2000**, *122*, 810. (b) Brady, M.; Weng, W.; Zhou, Y.; Seyler, J. W.; Amoroso, A. J.; Arif, A. M.; Böhme, M.; Frenking, G.; Gladysz, J. A. *J. Am. Chem. Soc.* **1997**, *119*, 775. (c) Jiao, H.; Costuas, K.; Gladysz, J. A.; Halet, J.-F.; Guillemot, M.; Toupet, L.; Paul, F.; Lapinte, C. *J. Am. Chem. Soc.* **2003**, *125*, 9511. (d) Horn, C. R.; Gladysz, J. A. *J. Eur. Inorg. Chem.* **2003**, 2211. (e) Horn, C. R.; Martin-Alvarez, J. M.; Gladysz, J. A. *Organometallics* **2002**, *21*, 5386.

10.1021/om050765l CCC: $33.50
Publication on Web 12/14/2005

$(CH{=}CH)_m{-}\{M\}$[18,19a,b] because of their facile accessibility and high efficiency for electronic delocalization. By contrast, extended molecular rods $\{M\}{-}C{\equiv}C{-}(CH{=}CH)_m{-}C{\equiv}C{-}\{M\}$ linked by a π-conjugated carbon chain with both ethynyl and ethenyl have comparatively been neglected.[2a,19c,d,20]

A judicious selection of redox-active organometallic termini is another critical point to electronic delocalization along the molecular backbone. It has been demonstrated that auxiliary ligands with different electronic effects could exert an important influence on the redox potential and wave splitting arising from electronic interaction.[2] To the best of our knowledge, most of the available redox-active organometallic components in the construction of polyynediyl or polyenediyl-bridged bimetallic complexes have 1+ charge, including $\{Cl(dppe)_2Ru\}^+$ (dppe = 1,2-bis(diphenylphosphino)ethane),[7] $\{Cp^*(dppe)Fe\}^+$,[10,18a] $\{X(dmpe)_2Mn\}^+$ (dmpe = 1,2-bis(dimethylphosphino)ethane, X = I, C≡CH),[12] $\{Cp^*(CO)_2Fe\}^+$,[14] $\{Cp(PPh_3)_2Ru\}^+$,[8a] $\{Cp(dppe)Ru\}^+$,[9b] $\{Cp^*(PP)Ru\}^+$ (PP = dppm, dppe),[8d] $\{Cp(dppf)Ru\}^+$ (dppf = 1,1′-bis(diphenylphosphino)ferrocene),[13] $\{Cp^*(NO)(PR_3)Re\}^+$ (R = aryl),[11] $\{Cl(PPr^i_3)_2HRh/Ir\}^+$,[15] $\{Cl(CO)(PPh_3)_3Ru\}^+$,[19] $\{M_2(ap)_4\}^+$ (ap = 2-anilinopyridinate anion) (M = Ru, Rh),[16,17] etc. Linkage of these organometallic components with polyynediyl or polyenediyl affords frequently the neutral homovalent molecular rods $\{M\}{-}(C{\equiv}C)_m{-}\{M\}$ or $\{M\}{-}(CH{=}CH)_m{-}\{M\}$. In this study, we attempt to utilize the 2+ organometallic component $\{(Phtpy)(PPh_3)_2Ru\}^{2+}$ as a redox terminus for the design of dicationic homovalent molecular rods $[\{(Phtpy)(PPh_3)_2Ru\}_2\{C{\equiv}C{-}(CH{=}CH)_m{-}C{\equiv}C\}]^{2+}$ (m = 0, 1, 2, 3) linked by a π-conjugated carbon chain with both ethynyl and ethenyl. We describe herein the syntheses, characterization, redox properties, and mixed-valence chemistry of this series of binuclear ruthenium complexes with extended π-conjugation.

Experimental Section

General Material. The manipulations were carried out in an atmosphere of dry argon by using standard Schlenk techniques and a vacuum-line system. The solvents were dried, distilled, and degassed before use except that those for UV−vis−NIR spectral measurements were of spectroscopic grade. The reagents ruthenium(III) chloride hydrate, 1,4-bis(trimethylsilyl)-1,3-butadiyne, silver perchlorate, and ferrocenium hexafluorophosphate were commercially available (Acros or Strem Chemicals). The compounds 4′-phenyl-2,2′:6′,2″-terpyridine (Phtpy),[21] $[(Ph\text{-}tpy)(PPh_3)_2RuCl](ClO_4)$,[22] (*E*)-$Me_3SiC{\equiv}C{-}CH{=}CH{-}C{\equiv}CSiMe_3$,[19c,23] (3*E*,5*E*)-$Me_3SiC{\equiv}C{-}CH{=}CH{-}CH{=}CH{-}C{\equiv}CSiMe_3$,[19a] and (3*E*,5*E*,7*E*)-$Me_3SiC{\equiv}C{-}CH{=}CH{-}CH{=}CH{-}CH{=}CH{-}C{\equiv}CSiMe_3$[24] were synthesized by the literature methods.

Caution! *Perchlorate salts are potentially explosive and should be handled carefully.*

$[\{(Phtpy)(PPh_3)_2Ru\}_2(C{\equiv}C{-}C{\equiv}C)](ClO_4)_2$ ($[1](ClO_4)_2$). $[(Phtpy)(PPh_3)_2RuCl](ClO_4)$ (150 mg, 0.14 mmol) and silver perchlorate (30.0 mg, 0.14 mmol) were dissolved in acetone (50 mL). After stirred under reflux for half an hour, the solution was cooled to room temperature and filtered to remove the silver chloride precipitate. To the brown filtrate were added 1,4-bis(trimethylsilyl)-1,3-butadiyne (14.0 mg, 0.07 mmol) and potassium fluoride (10 mg, 0.17 mmol). The solution was then stirred under reflux for 1 day to give a green residue by removing the solvent in vacuo. The product was purified by chromatography on a neutral alumina column using dichloromethane−acetone (10:1) as an eluent to collect the green band. Yield: 68%. Anal. Calcd for $C_{118}H_{90}Cl_2N_6O_8P_4Ru_2$: C, 66.95; H, 4.29; N, 3.97. Found: C, 66.69; H, 4.23; N, 3.84. ES-MS: *m*/*z* (%) 959 (100) $[M - (ClO_4)_2]^{2+}$, 983 (5) $[\{(Phtpy)(PPh_3)_2Ru\}(C{\equiv}C{-}C{\equiv}C)]^+$. IR (KBr, cm^{-1}): ν 1979m (C≡C), 1090s (ClO_4). ^1H NMR (CD_3CN, ppm): δ 9.04 (d, 4H, J = 7.5 Hz, tpy(6 6″)), 7.93 (d, 4H, J = 7.0 Hz, tpy(3 3″)), 7.79 (d of d, 4H, J = 11.5 Hz, J' = 7.5 Hz, tpy(4 4″)), 7.66 (s, 4H, tpy(3′ 5′)), 7.27−6.93 (m, 70H, C_6H_5, and 4H, tpy (5 5″)). ^{31}P NMR (CD_3CN): δ 28.0 (s). UV−vis (CH_3CN): λ_{max}/nm (ϵ/M^{-1} cm^{-1}) = 231 (260 600), 265 (173 700), 316 (119 200), 406 (23 170), 629 (22 300).

$[\{(Phtpy)(PPh_3)_2Ru\}_2(C{\equiv}C{-}CH{=}CH{-}C{\equiv}C)](ClO_4)_2$ ($[2](ClO_4)_2$). This compound was prepared by the same procedure as that of **[1]**$(ClO_4)_2$ except for using (*E*)-$Me_3SiC{\equiv}C{-}CH{=}CH{-}C{\equiv}CSiMe_3$ instead of 1,4-bis(trimethylsilyl)-1,3-butadiyne. Yield: 53%. Anal. Calcd for $C_{120}H_{92}Cl_2N_6O_8P_4Ru_2$: C, 67.26; H, 4.33; N, 3.92. Found: C, 67.13; H, 4.49; N, 3.93. ES-MS: *m*/*z* (%) 972 (100) $[M - (ClO_4)_2]^{2+}$, 1009 (5) $[\{(Phtpy)(PPh^3)Ru\}(C{\equiv}C{-}CH{=}CH{-}C{\equiv}C)]^+$. IR (KBr, cm^{-1}): ν 2031m (C≡C), 1697m (C=C), 1090s (ClO_4). ^1H NMR (CD_3CN, ppm): δ 9.11−7.08 (m, 90H, tpy and C_6H_5), δ 6.53 (s, 2H, CH=). ^{31}P NMR (CD_3CN): δ 29.4 (s). UV−vis (CH_3CN): λ_{max}/nm (ϵ/M^{-1} cm^{-1}) = 273 (223 400), 316 (155 100), 363 (83 200), 510 (25 300).

$[\{(Phtpy)(PPh_3)_2Ru\}_2(C{\equiv}C{-}CH{=}CH{-}CH{=}CH{-}C{\equiv}C)](ClO_4)_2$ ($[3](ClO_4)_2$). This compound was prepared by the same procedure as that of **[1]**$(ClO_4)_2$ except for the use of (3*E*,5*E*)-$Me_3SiC{\equiv}C{-}CH{=}CH{-}CH{=}CH{-}C{\equiv}CSiMe_3$ instead of 1,4-bis(trimethylsilyl)-1,3-butadiyne. Yield: 50%. Anal. Calcd for $C_{122}H_{94}Cl_2N_6O_8P_4Ru_2$: C, 67.56; H, 4.37; N, 3.87. Found: C, 67.26; H, 4.55; N, 3.57. ES-MS: *m*/*z* (%) 985 (100) $[M - (ClO_4)_2]^{2+}$, 1035-(13) $[\{(Phtpy)(PPh_3)_2Ru\}(C{\equiv}C{-}CH{=}CH{-}CH{=}CH{-}C{\equiv}C)]^+$. IR (KBr, cm^{-1}): ν 2022m (C≡C), 1697m (C=C), 1090s (ClO_4). ^1H NMR (CD_3CN, ppm): δ 9.09−7.27 (m, 90H, tpy and C_6H_5), 6.67 (m, 2H, C≡C−CH=C*H*−C*H*=CH−C≡C), 6.27 (m, 2H, C≡C−C*H*=CH−CH=C*H*−C≡C). ^{31}P NMR (CD_3CN): δ 29.6 (s). UV−vis (CH_3CN): λ_{max}/nm (ϵ/M^{-1} cm^{-1}) = 273 (145 540), 309 (99 200), 340 (50 900), 389 (57 450), 490 (26 220).

(12) (a) Kheradmandan, S.; Heinze, K.; Schmalle, H. W.; Berke, H. *Angew. Chem., Int. Ed*. **1999**, *38*, 2270. (b) Fernández, F. J.; Venkatesan, K.; Blacque, O.; Alfonso, M.; Schmalle, H. W.; Berke, H. *Chem. Eur. J*. **2003**, *9*, 6192.

(13) Gao, L.-B.; Zhang, L.-Y.; Shi, L.-X.; Chen, Z.-N. *Organometallics* **2005**, *24*, 1678.

(14) Akita, M.; Chung, M.-C.; Sakurai, A.; Sugimoto, S.; Terada, M.; Tanaka, M.; Moro-oka, Y. *Organometallics* **1997**, *16*, 4882.

(15) (a) Gil-Rubio, J.; Laubender, M.; Werner, H. *Organometallics* **2000**, *19*, 1365. (b) Gil-Rubio, J.; Laubender, M.; Werner, H. *Organometallics* **1998**, *17*, 1202. (c) Gevert, O.; Wolf, J.; Werner, H. *Organometallics* **1996**, *15*, 2806.

(16) (a) Xu, G.-L.; Zou, G.; Ni, Y.-H.; DeRosa, M. C.; Crutchley, R. J.; Ren, T. *J. Am. Chem. Soc*. **2003**, *125*, 10057. (b) Xu, G.-L.; DeRosa, M. C.; Crutchley, R. J.; Ren, T. *J. Am. Chem. Soc*. **2004**, *126*, 3728. (c) Wong, K.-T.; Lehn, J.-M.; Peng, S.-M.; Lee, G.-H. *Chem. Commun*. **2000**, 2259. (d) Xu, G.-L.; Crutchley, R. J.; DeRosa, M. C.; Pan, Q.-J.; Zhang, H.-X.; Wang, X.; Ren, T. *J. Am. Chem. Soc*. **2005**, *127*, 13354−13363.

(17) Bear, J. L.; Han, B.; Wu, Z.; Van Caemelbecke, E.; Kadish, K. M. *Inorg. Chem*. **2001**, *40*, 2275.

(18) (a) Chung, M. C.; Gu, X.; Etzenhouser, B. A.; Spuches, A. M.; Rye, P. T.; Seetharaman, S. K.; Rose, D. J.; Zubieta, J.; Sponsler, M. B. *Organometallics* **2003**, *22*, 3485. (b) Etzenhouser, B. A.; Cavanaugh, M. D.; Spurgeon, H. N.; Sponsler, M. B. *J. Am. Chem. Soc*. **1994**, *116*, 2221. (c) Etzenhouser, B. A.; Chen, Q.; Sponsler, M. B. *Organometallics* **1994**, *13*, 4176. (d) Sponsler, M. B. *Organometallics* **1994**, *13*, 1920.

(19) (a) Liu, S. H.; Chen, Y.; Wan, K. L.; Wen, T. B.; Zhou, Z.; Lo, M. F.; Williams, I. D.; Jai, G. *Organometallics* **2002**, *21*, 4984. (b) Liu, S. H.; Xia, H.; Wen, T. B.; Zhou, Z. Y.; Jia, G. *Organometallics* **2003**, *22*, 737. (c) Xia, H. P.; Ng, W. S.; Ye, J. S.; Li, X. Y.; Wong, W. T.; Lin, Z.; Yang, C.; Jia, G. *Organometallics* **1999**, *18*, 4552. (d) Xia, H. P.; Wu, W. F.; Ng, W. S.; Williams, I. D.; Jia, G. *Organometallics* **1997**, *16*, 2940.

(20) Shi, Y.; Yee, G. T.; Wang, G.; Ren, T. *J. Am. Chem. Soc*. **2004**, *126*, 10552.

(21) Constable, E. C.; Lewis, J.; Liptrot, M. C.; Raithby, P. R. *Inorg. Chim. Acta* **1990**, *178*, 47.

(22) Sullivan, B. P.; Calvert, J. M.; Meyer, T. J. *Inorg. Chem*. **1980**, *19*, 1404.

(23) Walker, J. A.; Bitler, S. P.; Wudl, F. *J. Org. Chem*. **1984**, *49*, 4733.

(24) Liu, S. H.; Hu, Q. Y.; Xue, P.; Wen, T. B.; Williams, I. D.; Jia, G. *Organometallics* **2005**, *24*, 769.

[{(Phtpy)(PPh$_3$)$_2$Ru}$_2$(C≡C−CH═CH−CH═CH−CH═CH−C≡C)](ClO$_4$)$_2$([4](ClO$_4$)$_2$). This compound was prepared by the same procedure as that of **[1]**(ClO$_4$)$_2$ except for using (3*E*,5*E*,7*E*)-Me$_3$SiC≡C−CH═CH−CH═CH−CH═CH−C≡CSiMe$_3$ instead of 1,4-bis(trimethylsilyl)-1,3-butadiyne. Yield: 46%. Anal. Calcd for $C_{124}H_{96}Cl_2N_6O_8P_4Ru_2$: C, 67.85; H, 4.41; N, 3.83. Found: C, 67.56; H, 4.63; N, 3.55. ES-MS: *m*/*z* (%) 998 (22) [M − (ClO$_4$)$_2$]$^{2+}$, 1061-(15) [{(Phtpy)(PPh$_3$)$_2$Ru}(C≡C−CH═CH−CH═CH−CH═CH−C≡C)]$^+$. IR (KBr, cm^{-1}): ν 2023m (C≡C), 1697m (C═C), 1638 (C═C), 1090s (ClO$_4$). ^{1}H NMR (CDCl$_3$, ppm): δ 9.03−7.06 (m, 90H, tpy and C$_6$H$_5$), 6.41 (m, 2H, ═CH−), 6.08 (m, 2H, ═CH−), 5.84 (m, 2H, −CH═). ^{31}P NMR (CD$_3$CN): δ 29.4 (s). UV−vis (CH$_3$CN): λ_{max}/nm (ϵ/M^{-1} cm^{-1}) = 277 (77 850), 322 (42 040), 432 (15 890).

[{(Phtpy)(PPh$_3$)$_2$Ru}$_2$(C≡C−C≡C)](ClO$_4$)$_2$(PF$_6$) ([1a](ClO$_4$)$_2$-(PF$_6$)). To a dichloromethane (20 mL) solution of **[1]**(ClO$_4$)$_2$ (50.0 mg, 0.024 mmol) was added ferrocenium hexafluorophosphate (8.0 mg, 0.024 mmol). The solution was stirred at 0 °C for half an hour with a color change from green into dark blue. After the solution was concentrated to leave 3 mL by evaporating the solvent, diethyl ether was added to produce a precipitate. After filtering, the precipitate was washed with 10 mL of diethyl ether three times. Yield: 85%. Anal. Calcd for $C_{118}H_{90}Cl_2F_6N_6O_8P_5Ru_2\cdot 2CH_2Cl_2$: C, 59.27; H, 3.90; N, 3.46. Found: C, 58.95; H, 4.08; N, 3.43. ES-MS: *m*/*z* (%) 639 (35) [M − (ClO$_4$)$_2$ − (PF$_6$)]$^{3+}$. IR (KBr, cm^{-1}): ν 1853s (C≡C), 1090s (ClO$_4$), 839s (PF$_6$). ^{31}P NMR (CD$_3$CN): δ 30.8 (s), −144.5 (septet, *P*F$_6$). UV−vis−NIR spectrum (CH$_2$Cl$_2$): λ_{max}/nm (ϵ/M^{-1} cm^{-1}) = 411 (20 360), 590 (12 410), 835 (16 300), 1005 (38 810).

[{(Phtpy)(PPh$_3$)$_2$Ru}$_2$(C≡C−CH═CH−C≡C)](ClO$_4$)$_2$(PF$_6$) ([2a](ClO$_4$)$_2$(PF$_6$)). The synthetic procedure of this compound was the same as that of **[1a]**(ClO$_4$)$_2$(PF$_6$) using **[2]**(ClO$_4$)$_2$ instead of **[1]**(ClO$_4$)$_2$ to give a mauve product. Yield: 92%. Anal. Calcd for $C_{120}H_{92}Cl_2F_6N_6O_8P_5Ru_2\cdot 2CH_2Cl_2$: C, 59.62; H, 3.94; N, 3.42. Found: C, 59.43; H, 4.41; N 3.45. ES-MS: *m*/*z* (%) 648 (82) [M − (ClO$_4$)$_2$ − (PF$_6$)]$^{3+}$. IR (KBr, cm^{-1}): ν 1979m (C≡C), 1090s (ClO$_4$), 838s (PF$_6$). ^{31}P NMR (CD$_3$CN): δ 33.1 (s), −144.6 (septet, *P*F$_6$). UV−vis−NIR (CH$_2$Cl$_2$): λ_{max}/nm (ϵ/M^{-1} cm^{-1}) = 430 (14 030), 505 (17 500), 889 (6630), 1069 (14 300).

[{(Phtpy)(PPh$_3$)$_2$Ru}$_2$(C≡C−CH═CH−CH═CH−C≡C)](Cl-O$_4$)$_2$(PF$_6$) ([3a](ClO$_4$)$_2$(PF$_6$)). The synthetic procedure of this compound was the same as that of **[1a]**(ClO$_4$)$_2$(PF$_6$) using **[3]**(ClO$_4$)$_2$ instead of **[1]**(ClO$_4$)$_2$ to give a blue product. Yield: 90%. Anal. Calcd for $C_{122}H_{94}Cl_2F_6N_6O_8P_5Ru_2\cdot 2CH_2Cl_2$: C, 59.96; H, 3.98; N, 3.38. Found: C, 60.43; H, 4.41; N 3.45. ES-MS: *m*/*z* (%) 657 (83) [M − (ClO$_4$)$_2$ − (PF$_6$)]$^{3+}$. IR (KBr, cm^{-1}): ν 1926m (C≡C), 1090s (ClO$_4$), 839s (PF$_6$). UV−vis−NIR (CH$_2$Cl$_2$): λ_{max}/nm (ϵ/M^{-1} cm^{-1}) = 408 (17 900), 503 (13 440), 679 (10 770), 755 (8030), 1171 (6850).

Crystal Structural Determination. Crystals of [**1**](PF$_6$)$_2$·H$_2$O (prepared by metathesis of perchlorate in **[1]**(ClO$_4$)$_2$ with potassium hexafluorophosphate) suitable for X-ray crystallography were grown by layering toluene onto the dichloromethane solution. A single crystal sealed in a capillary with mother liquor was measured on a SIEMENS SMART CCD diffractometer by ω scan technique at room temperature using graphite-monochromated Mo Kα (λ = 0.71073 Å) radiation. Absorption corrections by SADABS were applied to the intensity data. The structure was solved by direct methods, and the heavy atoms were located from an E-map. The remaining non-hydrogen atoms were determined from the successive difference Fourier syntheses. All non-hydrogen atoms were refined anisotropically, and the hydrogen atoms were generated geometrically and refined with isotropic thermal parameters. The structures were refined on F^2 by full-matrix least-squares methods using the SHELXTL-97 program package.[25] The crystallographic data are summarized in Table 1.

Table 1. Crystallographic Data for [1](PF$_6$)$_2$·H$_2$O

empirical formula	$C_{118}H_{92}F_{12}N_6OP_6Ru_2$
temp, K	293(2)
space group	*C*2/*c*
a, Å	39.214(3)
b, Å	13.1766(8)
c, Å	28.174(2)
β, deg	131.978(2)
V, Å^3	10822.2(14)
Z	4
ρ_{calcd}, g/cm^{-3}	1.366
μ, mm^{-1}	0.441
radiation (λ, Å)	0.71073
R1(F_o)[a]	0.0682
wR2(F_o)[b]	0.1973
GOF	1.099

[a] $R1 = \sum|F_o - F_c|/\sum F_o$. [b] $wR2 = \sum[w(F_o^2 - F_c^2)^2]/\sum[w(F_o^2)]^{1/2}$.

Physical Measurements. Elemental analyses were performed on a Perkin-Elmer Model 240C automatic instrument. The electrospray mass spectra (ES-MS) were recorded on a Finnigan LCQ mass spectrometer using dichloromethane−methanol as mobile phase. The UV−vis−NIR spectra were measured on a Perkin-Elmer Lambda 900 UV−vis−NIR spectrometer. The IR spectra were recorded on a Magna 750 FT-IR spectrophotometer using KBr pellets. The ^{1}H and ^{31}P NMR spectra were measured on a Varian UNITY-500 spectrometer with SiMe$_4$ as the internal reference and 85% H$_3$PO$_4$ as external standard, respectively. The cyclic voltammogram (CV) and differential pulse voltammogram (DPV) were made with a potentiostat/galvanostat Model 263A in dichloromethane solutions containing 0.1 M (Bu$_4$N)(PF$_6$) as supporting electrolyte. CV was performed at a scan rate of 100 mV s^{-1}. DPV was measured at a rate of 20 mV s^{-1} with a pulse height of 40 mV. Platinum and glassy graphite were used as counter and working electrodes, respectively, and the potential was measured against a Ag/AgCl reference electrode. The potential measured was always referenced to the half-wave potentials of the ferrocenium/ferrocene couple ($E_{1/2}$ = 0).

Results and Discussion

Syntheses and Characterization. As shown in Scheme 1, binuclear complexes [{(Phtpy)(PPh$_3$)$_2$Ru}$_2${C≡C−(CH═CH)$_m$−C≡C}]$^{2+}$ (m = 0, 1, 2, 3) were prepared in two steps. The chloride-containing complex [(Phtpy)(PPh$_3$)$_2$RuCl]$^+$ reacts first with silver perchlorate in refluxed acetone to facilitate dissociation of the Ru−Cl bond, producing the acetone-bound complex [(Phtpy)(PPh$_3$)$_2$Ru(acetone)]$^{2+}$. The desired products [**1**](ClO$_4$)$_2$−[**4**](ClO$_4$)$_2$ were then accessible via fluoride-catalyzed[8,13] desilylation of Me$_3$Si−C≡C−(CH═CH)$_m$−C≡C−SiMe$_3$ by reaction with [(Phtpy)(PPh$_3$)$_2$Ru(acetone)]$^{2+}$ in refluxed acetone for 1 day. Compound [**1**](ClO$_4$)$_2$ was isolated as a green solid, whereas [**2**](ClO$_4$)$_2$−[**4**](ClO$_4$)$_2$ as brown products with overall yields of 46−68%. The products could readily be purified by neutral alumina column chromatography and collected as the main band. The reactions were also carried out in acetonitrile or methanol, but usually afforded [**1**](ClO$_4$)$_2$−[**4**](ClO$_4$)$_2$ in lower yields. Oxidation of the Ru$_2^{II,II}$ complexes [**1**]$^{2+}$−[**3**]$^{2+}$ with 1 equiv of ferrocenium hexafluorophosphate afforded the stable Ru$_2^{II,III}$ mixed-valence complexes [**1a**]$^{3+}$−[**3a**]$^{3+}$, respectively. Attempts to prepare the Ru$_2^{III,III}$ complexes by further oxidation of [**1a**]$^{3+}$−[**3a**]$^{3+}$ with silver hexafluorophosphate (AgPF$_6$) or nitrosonium tetrafloroborate ([NO][BF$_4$]) were unsuccessful because of their instability even at low temperature.

The positive ion ESI-MS of compounds [**1**](ClO$_4$)$_2$−[**4**]-(ClO$_4$)$_2$ show molecular ion fragments [M − (ClO$_4$)$_2$]$^{2+}$ as the

(25) Sheldrick, G. M. *SHELXL-97, Program for the Refinement of Crystal Structures*; University of Göttingen: Göttingen, Germany, 1997.

Scheme 1. Synthetic Routes to $[\{(Phtpy)(PPh_3)_2Ru\}_2\{C{\equiv}C{-}(CH{=}CH)_m{-}C{\equiv}C\}]^{n+}$ (m = 0, 1, 2, 3; n = 2, 3)

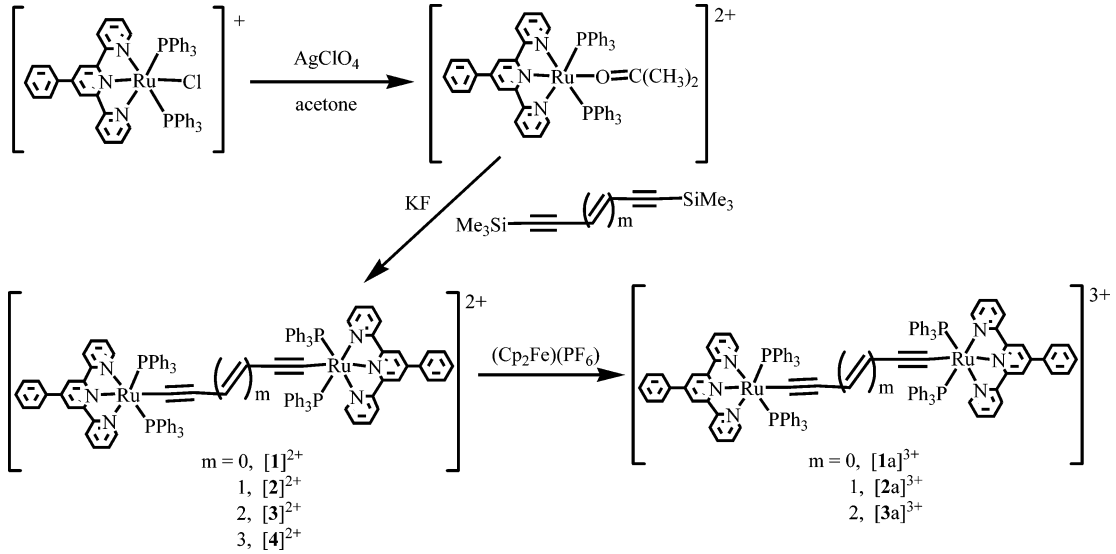

principal peaks. In the ESI-MS of $Ru_2^{II,III}$ mixed-valence compounds $[\mathbf{1a}](ClO_4)_2(PF_6)$−$[\mathbf{3a}](ClO_4)_2(PF_6)$, the molecular ion peaks $[M - (ClO_4)_2 - (PF_6)]^{3+}$ occur in high abundance. The IR spectra of complexes $[\mathbf{1}]^{2+}$−$[\mathbf{4}]^{2+}$ display ν(C≡C) bands at 1980−2025 cm^{-1} with moderate intensity. Upon one-electron oxidation, the ν(C≡C) frequency is remarkably red-shifted (60−120 cm^{-1}) in the mixed-valence $Ru_2^{II,III}$ complexes $[\mathbf{1a}]^{3+}$−$[\mathbf{3a}]^{3+}$. Obviously, the C≡C bonding is weakened with oxidation of the $Ru_2^{II,II}$ into $Ru_2^{II,III}$, reflecting a reduced bond order in the carbon chain and an increasing contribution from cumulenic resonance structures.[8−13] In the ^{31}P NMR spectra of $[\mathbf{1}](ClO_4)_2$−$[\mathbf{4}](ClO_4)_2$, only a singlet occurs at 28.0, 29.4, 29.6, and 29.4 ppm, respectively. This signal shifts to 30.9 and 33.1 ppm in the mixed-valence compounds $[\mathbf{1a}](ClO_4)_2(PF_6)$ and $[\mathbf{2a}](ClO_4)_2$-(PF_6), respectively. The phosphorus multiplets in hexafluorophosphate appear at ca. −144.0 ppm.

Crystal Structures. The structure of $[\mathbf{1}](ClO_4)_2$ was determined by X-ray crystallography. A perspective view of the complex cation $[\{(Phtpy)(PPh_3)_2Ru\}_2(C{\equiv}C{-}C{\equiv}C)]^{2+}$ is depicted in Figure 1. Relevant bond lengths and angles are listed in Table 2.

The complex cation consists of two $(Phtpy)(PPh_3)_2Ru$ units bridged by butadiynyl C≡C−C≡C through σ coordination. The Ru^{II} geometry can be described as an elongated octahedron composed of CN_3P_2 donors. The equatorial plane is built by three N donors of Phtpy and one C donor of alkynyl, and the axial sites are occupied by two trans-oriented P donors of PPh_3. The equatorial planes of Ru1 and Ru1A octahedrons are intercrossed with each other to form a dihedral angle of 49.3°. The $Ru{-}C_{acetylide}$ (2.000(5) Å) length is normal,[8b,d,13] while the Ru−P distances [2.3757(13) and 2.3725(12) Å] are a little longer

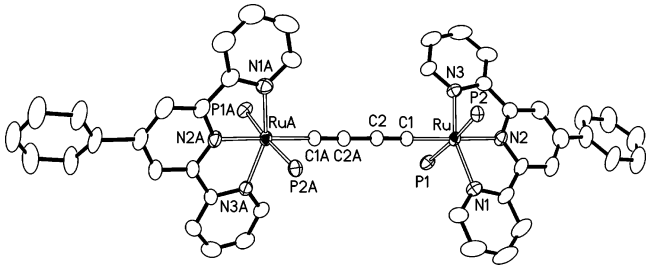

Figure 1. ORTEP drawing of $[\mathbf{1}]^{2+}$ with atom-labeling scheme showing 30% thermal ellipsoids. Phenyl rings on the phosphorus atoms are omitted for clarity.

Table 2. Selected Bond Distances (Å) and Angles (deg) for $[\mathbf{1}](PF_6)_2{\cdot}H_2O$

Ru−C1	2.000(5)	Ru−N1	2.095(4)
Ru−P1	2.3757(13)	Ru−N2	1.996(4)
Ru−P2	2.3725(12)	Ru−N3	2.084(4)
C1−C2	1.229(7)	C2−C2A	1.371(9)
P1−Ru−P2	173.38(4)	N2−Ru−C1	178.02(17)
C1−Ru−P1	85.66(13)	N2−Ru−N3	78.66(15)
C1−Ru−P2	87.72(12)	C1−Ru−N3	99.68(16)
C15−N3−Ru	113.4(3)	C1−Ru−N1	103.24(17)
N1−Ru−P1	89.53(12)	N3−Ru−N1	157.00(16)
N2−Ru−P1	93.26(12)	C21−N1−Ru	113.7(3)
N3−Ru−P1	90.32(11)	C16−N2−Ru	119.4(3)
N1−Ru−P2	91.77(12)	C11−N3−Ru	128.0(3)
N2−Ru−P2	93.36(12)	C2−C1−Ru	179.2(4)
N3−Ru−P2	91.00(11)	C1−C2−C2A	176.1(3)

than those found in the Cp or Cp* complexes $[\{Cp(PPh_3)_2Ru\}_2$-$(C{\equiv}C{-}C{\equiv}C)]$,[8b,9b] $[\{Cp^*(PP)Ru\}_2(C{\equiv}C{-}C{\equiv}C)]$ (PP = dppm, dppe),[8d] and $[\{Cp(dppf)Ru\}_2(C{\equiv}C{-}C{\equiv}C)]$.[13] The P−Ru−P, N−Ru−P, and N−Ru−N angles are comparable to those found in the mononuclear complex *trans*-$[Ru(Cl)(tpy)(PPh_3)_2]^+$.[26] The bridging array Ru−C≡C−C≡C−Ru is only a little distorted from linearity with the Ru−C≡C and C≡C−C angles being 179.2(4)° and 176.1(3)°, respectively. The C≡C length [1.229-(7) Å] is typical for carbon−carbon triple bonding.[8b,9b,13] The intramolecular Ru···Ru separation across the bridging C≡C−C≡C is 7.81 Å.

Electrochemistry. The redox chemsitry of compounds $[\mathbf{1}]$-$(ClO_4)_2$−$[\mathbf{4}](ClO_4)_2$ was investigated by cyclic and pulse differential voltammetry in a 0.1 M dichloromethane solution of $(Bu_4N)(PF_6)$. The electrochemical data are presented in Table 3, and plots of the cyclic voltammogram (CV) and pulse differential voltammogram (DPV) for compounds $[\mathbf{1}](ClO_4)_2$−$[\mathbf{4}](ClO_4)_2$ are depicted in Figure 2.

The mononuclear Ru^{II} complex $\{(Ph\text{-}tpy)Ru(PPh_3)_2Cl\}$-$(ClO_4)$[22,26a] exhibits a quasi-reversible redox wave at $E_{1/2}$ = +0.502 V (referenced to Fc^+/Fc) and an irreversible wave at $E_{1/2}$ = −1.908 V in dichloromethane solutions containing 0.1 M $(Bu_4N)(PF_6)$ as supporting electrolyte. The quasi-reversible wave on the anodic side can be assigned as metal-centered Ru^{II}/

(26) (a) Perez, W. J.; Lake, C. H.; See, R. F.; Toomey, L. M.; Churchill, M. R.; Takeuchi, K. J.; Radano, C. P.; Boyko, W. J.; Bessel, C. A. *J. Chem. Soc., Dalton Trans.* **1999**, 2281. (b) Sharma, S.; Singh, S. K.; Chandra, M.; Pandey, D. S. *J. Inorg. Biochem.* **2005**, *99*, 458.

Table 3. Electrochemical Data for Compounds [1](ClO$_4$)$_2$−[4](ClO$_4$)$_2$[a]

compound	$E_{1/2}$(A)	$E_{1/2}$(B)	$E_{1/2}$(C)	$\Delta E_{1/2}$[b]	K_c[c]	E_{pc}(Phtpy)[d]
[(Phtrpy)Ru(PPh$_3$)$_2$Cl](ClO$_4$)		+0.502				−1.908
[**1**](ClO$_4$)$_2$	−0.276	+0.334	+0.938	0.610	2.05×10^{10}	−2.030
[**2**](ClO$_4$)$_2$	−0.205	+0.055		0.260	2.48×10^4	−1.928
[**3**](ClO$_4$)$_2$	−0.184	−0.019		0.165	6.15×10^2	−1.911
[**4**](ClO$_4$)$_2$		−0.089		<0.070	<15	−1.885

[a] Potential data in volts vs Fc^+/Fc are from single-scan cyclic voltammograms recorded at 25 °C in a 0.1 M dichloromethane solution of (Bu_4N)(PF_6). Detailed experimental conditions are given in the Experimental Section. [b] $\Delta E_{1/2} = E_{1/2}(B) - E_{1/2}(A)$ denotes the potential difference between redox processes A and B. [c] The comproportionation constants, K_c, were calculated by the formula $K_c = \exp(\Delta E_{1/2}/25.69)$ at 298 K.[27] [d] It originates from the irreversible reduction of the Phtpy ligand.

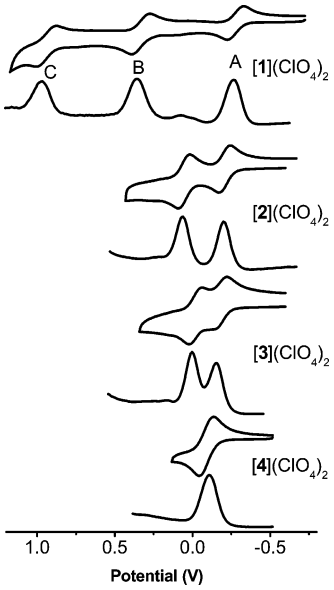

Figure 2. Cyclic and differential pulse voltammograms (CV and DPV) of compounds [**1**](ClO$_4$)$_2$−[**4**](ClO$_4$)$_2$ in a 0.1 M dichloromethane solution of (Bu_4N)(PF_6). The scan rate is 100 mV s^{-1} for CV and 20 mV s^{-1} for DPV.

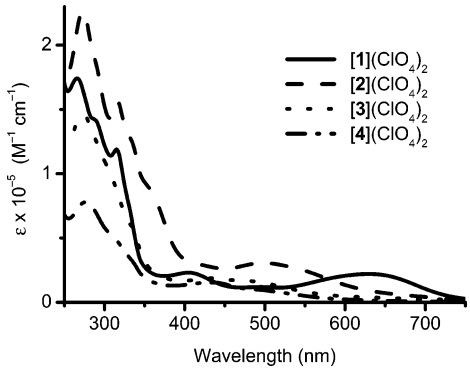

Figure 3. UV−vis spectra of [**1**](ClO$_4$)$_2$ (solid line), [**2**](ClO$_4$)$_2$ (dashed line), [**3**](ClO$_4$)$_2$ (dotted line), and [**4**](ClO$_4$)$_2$ (dash−dot line) in acetonitrile.

Ru^{III} oxidation, while the irreversible wave in the cathodic region arises from reduction of the Phtpy ligand. This reduction wave is also observed in the binuclear ruthenium compounds [**1**](ClO$_4$)$_2$−[**4**](ClO$_4$)$_2$ at $E_{1/2}$ = −2.030, −1.928, −1.911, and −1.885 V, respectively.

As indicated in Figure 2, the CV and DPV of compound [**1**](ClO$_4$)$_2$ exhibit three reversible redox waves at −0.276 (A), +0.334 (B), and +0.938 V (C), ascribed tentatively to the redox processes $[Ru_2]^{2+}/[Ru_2]^{3+}$, $[Ru_2]^{3+}/[Ru_2]^{4+}$, and $[Ru_2]^{4+}/[Ru_2]^{5+}$, respectively.[8a,d,13] Among them, waves A and B originate from stepwise one-electron oxidation of the $[Ru_2^{II,II}]^{2+}$ complex to $[Ru_2^{II,III}]^{3+}$ and $[Ru_2^{III,III}]^{4+}$ species, respectively. The large wave separation ($\Delta E_{1/2}$ = 0.610 V) between waves A and B suggests a significantly electronic delocalization along the molecular rod. The comproportionation constant K_c[27] (2.05×10^{10}) is quite large and indicative of strong metal−metal coupling. The $\Delta E_{1/2}$ and K_c values of [**1**](ClO$_4$)$_2$ are comparable to those of the butadiynyl-bridged binuclear ruthenium analogue {Cp(PPh$_3$)$_2$Ru}$_2$(C≡C−C≡C)[8d,9b] capped with Cp instead of Phtpy. Consequently, although Phtpy acts as a tridentate N_3 ligand via σ bonding, it functions in the same manner as that of Cp via η^5-π-coordination.

Compared with three reversible one-electron oxidation processes in [**1**](ClO$_4$)$_2$, only two one-electron oxidation waves are observed in the CV and DPV of [**2**](ClO$_4$)$_2$ and [**3**](ClO$_4$)$_2$ due to stepwise oxidation of $[Ru_2^{II,II}]^{2+}$ into $[Ru_2^{II,III}]^{3+}$ and $[Ru_2^{II,III}]^{3+}$ into $[Ru_2^{III,III}]^{4+}$, respectively. The wave separations $\Delta E_{1/2}$ between the two stepwise one-electron processes are 0.260 and 0.165 V, corresponding to $K_c = 2.48 \times 10^4$ and 6.15×10^2 for [**2**](ClO$_4$)$_2$ and [**3**](ClO$_4$)$_2$, respectively. By contrast, only one broad redox wave occurs at −0.089 V for [**4**](ClO$_4$)$_2$, revealing that the two closely spaced one-electron oxidations are unresolvable by CV and DPV. The $\Delta E_{1/2}$, which can be calculated from the width of this peak by the method of Richardson and Taube,[27] is lower than 0.07 V, with a comproportionation constant K_c < 15. By comparison of the $\Delta E_{1/2}$ values in [**1**](ClO$_4$)$_2$−[**4**](ClO$_4$)$_2$ (Table 3), it is demonstrated distinctly that electronic delocalization in the binuclear complexes [{(Phtpy)(PPh$_3$)$_2$Ru}$_2${C≡C−(CH=CH)$_m$−C≡C}]$^{2+}$ (m = 0, 1, 2, 3) decays dramatically with the increase of the ethenyl number in the bridging ligand C≡C−(CH=CH)$_m$−C≡C. The $\Delta E_{1/2}$ dependence on metal−metal distance is much more notable than that found in polyynediyl-bridged binuclear rhenium complexes {Cp*(NO)(PPh$_3$)Re}$_2$(C≡C)$_m$ (m = 1−10)[11a] and binuclear iron complexes {Cp*(dppe)Fe}$_2$(C≡C)$_m$ (m = 2, 4, 6),[2c] in which the $\Delta E_{1/2}$ reduces more slowly with an increase in ethynyl number.

UV−Vis−NIR Spectra. The UV−vis spectra of complexes [**1**]$^{2+}$−[**4**]$^{2+}$ in acetonitrile show a series of ligand-centered $\pi \rightarrow \pi^*$ transitions with high intensity in the UV region. The broad absorption bands with low energy at 380−630 nm originate from dπ(Ru) → π^*(Phtpy) metal-to-ligand charge transfer (MLCT) transitions.[22,26a,28] As shown in Figure 3, the MLCT bands exhibit a remarkable shift to higher energy with an increase in ethenyl number, and the energy sequence is [**1**]$^{2+}$ < [**2**]$^{2+}$ < [**3**]$^{2+}$ < [**4**]$^{2+}$. As the ethenyl number increases, the π electron-accepting ability in the bridging ligand C≡C−(CH=CH)$_m$−C≡C is enhanced, which would reduce the π electron density of the Ru^{II} centers and lower the energy of the dπ(Ru) orbital, thus raising the consequent energy gap between dπ(Ru) and

(27) Richardson, D. E.; Taube, H. *Inorg. Chem.* **1981**, *20*, 1278.

(28) Gagliardo, M.; Dijkstra, H. P.; Coppo, P.; De Cola, L.; Lutz, M.; Spek, A. L.; van Klink, G. P. M.; van Koten, G. *Organometallics* **2004**, *23*, 5833.

Table 4. Visble−Near-Infrared Spectral Data for $Ru_2^{II,III}$ Mixed-Valence Complexes $[1a]^{3+}$, $[2a]^{3+}$, and $[3a]^{3+}$ in Acetonitrile at 298 K

compound	λ_{max} (nm)	ϵ_{max} (cm^{-1} M^{-1})	ν_{max} (cm^{-1})	$\Delta\nu_{obsd}$ (cm^{-1})[a]	$\Delta\nu_{calcd}$ (cm^{-1})[b]	V_{ab}' (eV)[c]	V_{ab} (eV)[d]
$[\mathbf{1a}]^{3+}$	1005	38 810	9950	1776	3409	0.269	0.62
$[\mathbf{2a}]^{3+}$	1069	14 310	9354	2487	4095	0.145	0.58
$[\mathbf{3a}]^{3+}$	1171	6850	8540	3440	4089	0.091	0.53

[a] $\Delta\upsilon_{obsd}$ is the observed half-width of the IVCT band. [b] $\Delta\upsilon_{calcd}$ is the calculated half-width from the equation $\Delta\nu_{1/2} = (2310\nu_{max})^{1/2}$ by Hush's theoretical analysis. [c] $V_{ab}' = \{[2.05 \times 10^{-2}(\nu_{max}\epsilon_{max}\Delta\upsilon_{1/2})^{1/2}]/R\}$ from Hush's theoretical analysis for weakly coupling systems of class II mixed-valence compounds, where ϵ_{max}, ν_{max}, and $\Delta\upsilon_{1/2}$ are the molar extinction coefficient, the absorption maximum in wavenumber, and the bandwidth at half-maximum height in wavenumber, respectively; the metal−metal distances R are 7.8, 10.1, and 12.5 Å in $[\mathbf{1a}]^{3+}$, $[\mathbf{2a}]^{3+}$, and $[\mathbf{3a}]^{3+}$, respectively. [d] $V_{ab} = \nu_{max}/2$ for electronically delocalized class III mixed-valence compounds.

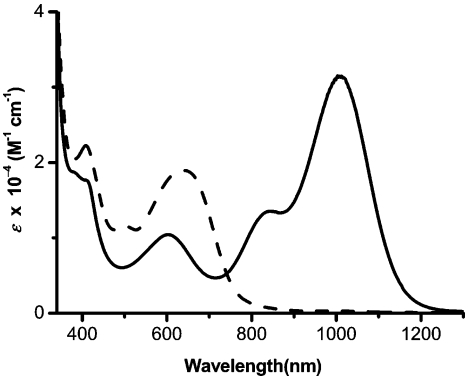

Figure 4. Visible−near-infrared spectra of $[\mathbf{1}]^{2+}$ (dashed line) and $[\mathbf{1a}]^{3+}$ (solid line) in dichloromethane, showing the IVCT band of the mixed-valence complex $[\mathbf{1a}]^{3+}$.

π^*(Phtpy) orbitals and inducing a blue shift of the MLCT absorption band.

In the UV−vis−NIR spectra of $Ru_2^{II,III}$ mixed-valence species $[\mathbf{1a}]^{3+}$−$[\mathbf{3a}]^{3+}$, the intensity of the dπ(Ru) → p*(Phtpy) MLCT band decreases markedly compared with that in the $Ru_2^{II,II}$ complexes $[\mathbf{1}]^{2+}$−$[\mathbf{3}]^{2+}$. Furthermore, a new lower energy band occurs at 750−890 nm (Figure 4) in the $Ru_2^{II,III}$ mixed-valence complexes $[\mathbf{1a}]^{3+}$−$[\mathbf{3a}]^{3+}$, ascribed tentatively to a ligand → Ru^{III} LMCT transition.[13]

Comparison of the electronic absorption spectra of the mixed-valence $Ru_2^{II,III}$ complexes $[\mathbf{1a}]^{3+}$−$[\mathbf{3a}]^{3+}$ with those of the $Ru_2^{II,II}$ species $[\mathbf{1}]^{2+}$−$[\mathbf{3}]^{2+}$, it is shown that $[\mathbf{1a}]^{3+}$−$[\mathbf{3a}]^{3+}$ show strong intervalence charge-transfer (IVCT) bands in the visible to near-infrared region, originating from the electronic transitions from the Ru^{II} to Ru^{III} centers. Figure 4 depicts the visible and near-infrared absorption spectra of $[\mathbf{1}]^{2+}$ and $[\mathbf{1a}]^{3+}$ measured in dichloromethane at 298 K, showing the characteristic IVCT band in mixed-valence complex $[\mathbf{1a}]^{3+}$. As listed in Table 4, this band is observed at 1005 nm for $[\mathbf{1a}]^{3+}$ with extinction coefficient $\epsilon = 38\,810$ M^{-1} cm^{-1}. Solvent independence of the λ_{max} values in the solvents such as dichloromethane, acetone, acetonitrile, and methanol with a wide range of polarity is distinctly indicative of the averaged solvation. Moreover, the observed half-width $\Delta\nu_{1/2}$ (1776 cm^{-1}) is significantly narrower than the widths (3409 cm^{-1}) calculated from the relationship in the equation $\Delta\nu_{1/2} = (2310\nu_{max})^{1/2}$, established by Hush for class II mixed-valence systems.[29] In view of these redox and absorption spectral features such as large comproportionation constant ($K_c = 2.05 \times 10^{10}$), high peak intensity ($\epsilon = 38\,810$ M^{-1} cm^{-1}), narrow half-width ($\Delta\nu_{1/2}$), and solvent independence of the IVCT band, it can be concluded that $Ru_2^{II,III}$ complex $[\mathbf{1a}]^{3+}$ are characteristic of a class III mixed-valence behavior with electronic delocalization.[30−35] Consequently, $[\mathbf{1a}]^{3+}$ is a typical class III mixed-valence complex according to Robin and Day classification.[31] The odd electron is delocalized over the Ru^{II}−C_4−Ru^{III} array, and the coupling parameter V_{ab} is simply related to the energy of the NIR band by $V_{ab} = \nu_{max}/2$.[8a,d,10b,13] The large V_{ab} (0.62 eV) of $[\mathbf{1a}]^{3+}$ is also suggestive of a typical class III mixed-valence behavior.

The C_6-bridged $Ru_2^{II,III}$ complex $[\mathbf{2a}]^{3+}$ exhibits broader and weaker IVCT bands than that of $[\mathbf{1a}]^{3+}$, but it also shows some characters of a class III mixed-valence complex. The IVCT band affords high intensity ($\epsilon = 14\,310$ cm^{-1} M^{-1}) and is independent of the solvent polarity. As listed in Table 4, the measured half-width (2487 cm^{-1}) is markedly narrower than the theoretical value (4095 cm^{-1}) calculated by Hush's theory for class II mixed-valence compounds.[29−31] Although the much lower $\Delta E_{1/2}$ (0.260 V) and K_c (2.48×10^4) values for $[\mathbf{2a}]^{3+}$ relative to those ($\Delta E_{1/2} = 0.610$ V, $K_c = 2.05 \times 10^{10}$) for $[\mathbf{1a}]^{3+}$ reveal a weaker electronic interaction between Ru^{II} and Ru^{III} across bridging C≡C−CH═CH−C≡C in $[\mathbf{2a}]^{3+}$, the IVCT features including its high intensity and solvent independence together with the narrow half-width suggest that it is not a typical class II mixed-valence complex. Consequently, $[\mathbf{2a}]^{3+}$ likely belongs to an intermediate between a valence-delocalized and valence-trapped system.

In contrast with $[\mathbf{1a}]^{3+}$ and $[\mathbf{2a}]^{3+}$, the mixed-valence complex $[\mathbf{3a}]^{3+}$ is unstable in dichloromethane and methanol at room temperature. The much weaker and broader IVCT band measured in acetonitrile occurs at 1171 nm with $\epsilon_{max} = 6850$ cm^{-1} M^{-1}. The measured half-width (3440 cm^{-1}) is not far from the theoretical value (4089 cm^{-1}) calculated by the equation $\Delta\nu_{1/2} = (2310\nu_{max})^{1/2}$.[29−31] Therefore, in terms of the IVCT band properties such as low intensity and broad half-width of the IVCT band together with the low K_c (6.15×10^2) value, it is suggested that $[\mathbf{3a}]^{3+}$ is a typical Robin−Day class II mixed-valence complex with weakly electronic coupling between Ru^{II} and Ru^{III} spanning the C≡C−CH═CH−CH═CH−C≡C carbon chain.

Conclusions

A series of sp and sp^2 carbon chain bridged $Ru_2^{II,II}$ complexes and their one-electron-oxidized $Ru_2^{II,III}$ species with mixed-valence were prepared utilizing $[(Phtpy)(PPh_3)_2Ru(acetone)]^{2+}$ as redox termini. It has been demonstrated that electronic delocalization in the complexes $[\{(Phtpy)(PPh_3)_2Ru\}_2\{C{\equiv}C-(CH{=}CH)_m-C{\equiv}C\}]^{3+}$ ($m = 0, 1, 2$) reduces dramatically with an increase in ethenyl number. The $Ru_2^{II,III}$ complex $[\mathbf{1a}]^{3+}$ (*m*

(29) Hush, N. S. *Prog. Inorg. Chem.* **1967**, *8*, 391.
(30) Richardson, D. E.; Taube, H. *Coord. Chem. Rev.* **1984**, *60*, 107−129.
(31) Robin, M. B.; Day, P. *Adv. Inorg. Chem. Radiochem.* **1967**, *10*, 247.
(32) Demadis, K. D.; Hartshorn, C. M.; Meyer, T. J. *Chem. Rev.* **2001**, *101*, 2655−2686.
(33) Brunschwig, B. S.; Creutz, C.; Sutin, N. *Chem. Soc. Rev.* **2002**, *31*, 168−184.
(34) Nelsen, S. F. *Chem. Eur. J.* **2000**, *6*, 581−588.
(35) Rezvani, A. R.; Bensimon, C.; Cromp, B.; Reber, C.; Greedan, J. E.; Kondratiev, V. V.; Crutchley, R. J. *Inorg. Chem.* **1997**, *36*, 3322−3329.

$= 0$) is characteristic of a class III mixed-valence system with electronic delocalization. The IVCT absorption together with the redox properties of $[\mathbf{2a}]^{3+}$ ($m = 1$) reveals that it is between electronically delocalized and valence-trapped. By contrast, $[\mathbf{3a}]^{3+}$ shows a typical Robin−Day class II mixed-valence behavior.

Acknowledgment. This work was supported by NSFC (Grants 20273074, 90401005, and 20490210), NSF of Fujian Province (E0420002 and E0310029), and the National Basic Research Program (Grant 001CB108906) of China.

Supporting Information Available: Visible−near-infrared spectra of mixed-valence compounds $[\mathbf{2a}](ClO_4)_2(PF_6)$ and $[\mathbf{3a}](ClO_4)_2(PF_6)$; X-ray crystallographic file in CIF format for the structure determination of compound $[\mathbf{1}](PF_6)_2 \cdot H_2O$. This material is available free of charge via the Internet at http://pubs.acs.org.

OM050765L